Supplemental Information for: Stabilization of Cationic Aluminum Hydroxide Clusters in High pH Environments with a $CaCl_2$/L-Arginine Matrix†

Scott E. Smart,[a,b] Viktor Dubovoy,[a] and Long Pan[a*]

Contents

[a] *Colgate-Palmolive Company, 909 River Road, Piscataway, NJ 08855, USA.*
[b] *Department of Chemistry and The James Franck Institute, The University of Chicago, Chicago, IL 60637, USA.*

1 Details Regarding Non-Acidic Aluminum Synthesis

Herein we report information regarding our synthesis of the non-acidic Al_{13} system (NAS_{13}), and then our investigations with other amino acids and aluminum species besides the $\varepsilon-Al_{13\text{-mer}}$ Keggin molecule.

1.1 Comments on the NAS_{13} Synthesis

Hydrolysis of aluminum at $[OH^-]$:$[Al^{3+}]$ ratios of above 2, and particularly at high concentrations of Al or base, easily result in the formation of a gelatinous aluminum hydroxide. For our stabilized system, we found that it was necessary to either: 1) have an $Al_{13\text{-mer}}$ solution (acidic) and add $CaCl_2$ and L-arginine (or, referred to as Arg) powder, or preferably; or 2) make an $Al_{13\text{-mer}}/CaCl_2$ solution and add L-arginine to it to yield a clear solution without any gelation. The results can be seen in Supplemental Figure 1. In the absence of $Al_{13\text{-mer}}$, the L-arginine and calcium system is highly soluble, and we were able to achieve a hydrated ionic liquid-like mixture through addition of concentrated hydrochloric acid to solid calcium chloride and L-arginine. Attempts to substitute calcium(II) with magnesium(II), sodium(I), or potassium(I) chloride salts were not effective, as the salts did not from soluble complexes with L-arginine across a wide pH range. L-lysine was found to work as a suitable substitute for L-arginine (see below), but other amino acids (L-histidine, L-alanine, etc.) were not found to be stable.

1.2 Other Compatible Amino-Acids

As mentioned above, L-lysine served as a good substitute for L-arginine, and can achieve more concentrated solutions due to its lower molecular weight. As such, the resulting pH in the concentrated or dilute solution was often higher than with L-arginine. Another system where the precursor was the $Al_{30\text{-mer}}$ with glycine,[1] and L-arginine was

Supplemental Fig. 1 The effective synthesis of stabilized ε-$Al_{13\text{-mer}}$ solution. Black lines represent components of system A, while blue dotted paths represent components of system B. % H_2O refers to percentage of total H_2O added, and the total % H_2O (w/w) in solution is constant at 45%. The molar ratio of $[Al^{3+}]$:$[CaCl_2 \cdot 2H_2O]$:[Arg] used here is 0.83:1:1

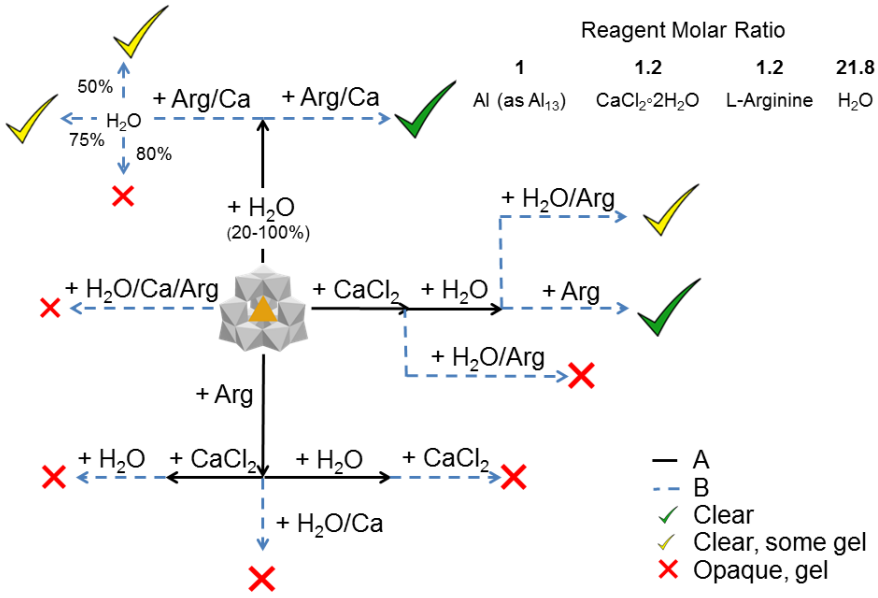

added also showed positive zeta potential at all amino acids concentrations, regardless of pH levels (there was no minimum required amount of L-arginine necessary). In addition, flocculation studies with 1% bovine serum albumin solutions showed the ability of these actives to neutralize and create floc. In addition, with these $Al_{30\text{-mer}}$ species, SEC showed only A/K/S peaks, meaning they also fall within the typical size ranges as their non-Ca/Arg counterparts. It is clear then that these samples were also in fact still partially hydrolyzed aluminum salts. With the exception of one system, namely $AlCl_3$ with Ca/Arg, all the samples showed similar characteristics. In all of these cases the complete and full hydrolysis of a partially hydrolyzed aluminum species to the corre-

sponding $Al(OH)_3$ form was being prevented in this system.

1.3 Experiments with Differing Aluminum Materials

1.3.1 Aluminum Chloride

One avenue of research was in looking at comparisons with previous work where L-arginine and $AlCl_3$ were used to create nano-$Al(OH)_3$. Measured pH values of samples containing varied L-arginine to aluminum molar ratios with Ca/Al molar ratio 1.2 is illustrated in Supplemental Figure 2. A comparative data set without L-arginine was obtained from previous work.[2] The samples without calcium exhibited a higher propensity for gel formation, especially at Arg/Al range between 2.10 - 2.30 where an opaque gel was the predominant phase. On the contrary, the samples containing calcium were all free-flowing liquids with slight gel phase formation at Arg/Al value of 2.40.

L-arginine's acid-base properties are best described as a zwitterion due to its combination of carboxylic acid (pKa = 2.17), α-amino (pKa = 9.04), and guanidinium (pKa = 12.48) functional groups with an isoelectric point of 10.76.The guanidine group (*i.e.*, CH_4N_3-R), and to a lesser extent α-amino (*i.e.*, R-NH_2) group, is largely responsible for the alkalinity of L-arginine due to its ability to deprotonate water to form hydroxide ions (Schematic 1). The guanidinium conjugate acid is a highly stable +1 cation in water due to the resonance stabilization and efficient solvation, which disperses the positive charge throughout all of nitrogen atoms. As a result of this alkalinity, L-arginine can act as a relatively mild source of hydroxide ions to facilitate a more gradual hydrolysis pathway as compared to strong bases.

For concentrations below the maximum soluble amount of L-arginine, increased L-arginine ratios resulted in the formation of P1 and P2, likely insoluble and large aggregate $Al(OH)_3$, similar to other work.[2] At higher aluminum concentrations Ca^{2+} caused

Supplemental Fig. 2 pH values of samples comprising aluminum chloride, calcium chloride, and L-arginine at varied L-arginine to aluminum ratios. Data set shown in black was obtained from previously published data.[2]

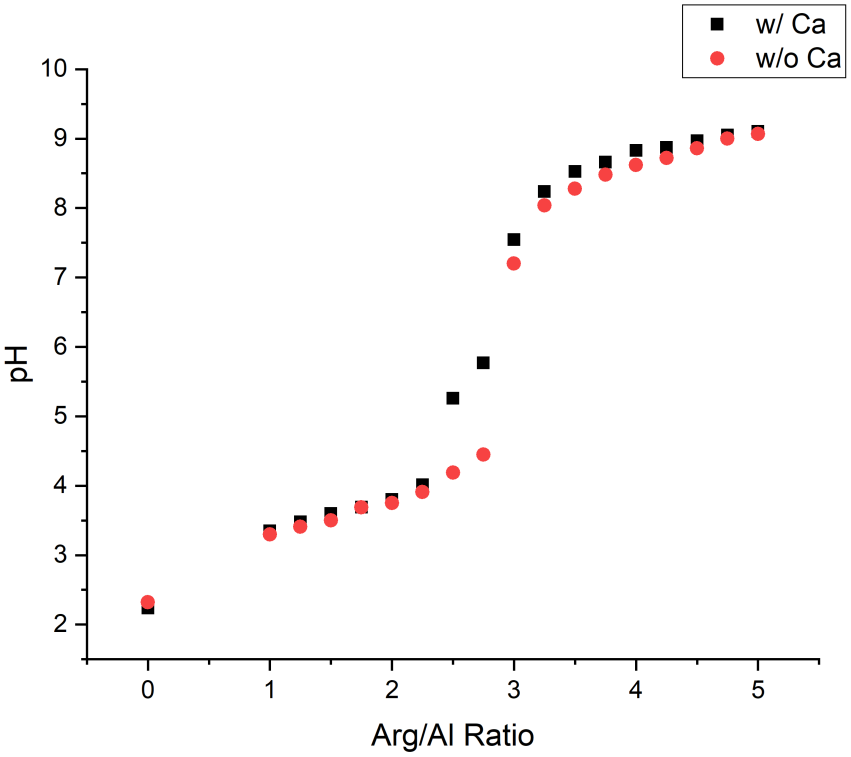

an increase in K peak (Keggin) at all Arg:Al ratios when compared with Dubovoy et al. At an Arg:Al ratio of 2.7-2.8, peak L emerges with K, and in general a very odd speciation is presented. As the Arg:Al ratio increases past 2.7, K species degrades into A, L, and mostly S, *i.e.* a mixture of some very large but mostly small Al units. It is also notable that as Al concentration increases to 2.4% Al from 0.6% Al at Arg:Al ratios of 2.8, L decreases, indicating that higher concentrations prevent the formation of large clusters. This could be due to charge repulsion and the viscous nature of the solution preventing monomeric addition of Al. As the Arg:Al ratio increases above 2.8 at all con-

Supplemental Fig. 3 Base ionization equilibrium for the guanidine group in L-arginine.

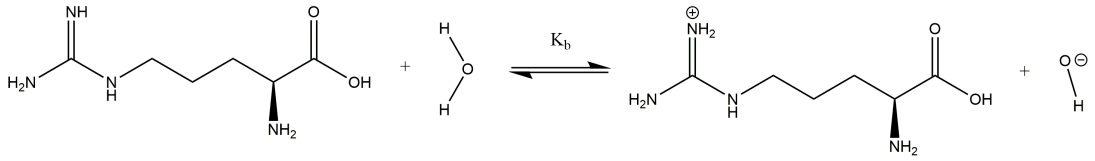

centrations, peak S forms again, becoming the major species. $AlCl_3$ at this point seems to have two pathways. One pathway leads to the growth of $Al(OH)_3$ nano-particles, confirmed in other work. Another pathway involves coordination of L-arginine to form small species such as $Al(OH)_2(HArg)^{2+}$, $Al(OH)_2(H_2Arg)_2^{3+}$, or $Al(OH)_3(H_2Arg)^{+}$, or possibly coordinated structures with dimers and trimers.

To contrast this, a mixture of $AlCl_3$ and $CaCl_2$ was made so that the Arg:Al molar ratio was 2.32. The experiment was aged for two days and SEC showed 100% peak K, referred to as sample κ. More L-arginine was added to κ to reach Arg:Al ratios of 2.5-3, and the samples were reacted for three days. SEC results were similar to the heated samples of $Al_{13\text{-mer}}$: A, mostly K, and small S, indicating that these samples had formed more stable species that did not undergo rapid polymerization.

The SEC results of the $AlCl_3$ system and a comparison with Dubovoy et al.[2] give the impression that methodical hydrolysis was occurring depending on the starting ratio of L-arginine and aluminum. Between a ratio of 2.6 and 2.8 Arg:Al the molecules agglomerate and form large nano-$Al(OH)_3$ species, such as P1 (L+). But, below this ratio, more controlled synthesis are possible. By keeping the Arg:Al ratio at an optimal level, we first created a pre-hydrolyzed species, which then was possible to then stabilize it with more L-arginine in a way similar as to $Al_{13\text{-mer}}$. The Keggin-sized structure then is an important component in effectively stabilizing this system.

For the most part, the titration-like curve illustrated in Supplemental Figure 2 demon-

strates only a slight variation in pH in presence of calcium chloride. Calcium chloride is not expected to exhibit significant acid or base properties since it can be described as a neutral salt derived from neutralization of strong base and acid (*i.e.*, calcium hydroxide and hydrochloric acid). However, significant differences in pH values were observed near the inflection point (ca. Arg/Al = 2.75) as a result of calcium chloride presence. A more detailed pH investigation (not shown) in the Arg/Al range of 2.10 – 3.40 demonstrates that in the range of Arg/Al 2.60 – 2.90 the samples comprising calcium exhibited pH values 0.90-1.20 higher than the samples without calcium. The significant increase in pH cannot be attributed to the acid-base properties of the neutral calcium chloride salt, which causes only a slight (*i.e.*, 0.25-0.55) deviation in pH at all other Arg/Al ratios. Moreover, the presence of calcium chloride at Arg/Al value of 2.90 brings the pH from a slightly acidic (pH = 5.70) to a neutral (pH = 6.90) environment without inducing precipitation of aluminum. These pH results further support the proposed stabilization of aluminum clusters in presence of L-arginine and calcium chloride.

1.3.2 Commerical Partially Hydrolyzed Materials

Similar experiments to the ones above were carried out where the source of aluminum was partially hydrolyzed aluminum materials, such as aluminum chlorohydrate (ACH), effective ACH (EACH), and others (see experiments with glycine and L-arginine). A similar effect is seen, *i.e.* - a partially hydrolyzed, positively charged aluminum species can be stabilized with the addition of calcium and L-arginine. Major differences were in the SEC results, which is expected as the starting speciation is much more polydisperse than in $AlCl_3$ or in the $Al_{13\text{-mer}}$ molecule.

2 Details Regarding Methodology

Herein we report some details on the different characterization methods used for our system and provide background information on some of the methods.

2.1 Comments on ζ-Potential

Because ζ-potential is not a direct measure of surface charge, but only of the potential difference between stationary layer of charges attached to the molecules and the solution, it is difficult to say whether the undiluted clusters themselves were still charged clusters. For instance, in turbidity tests, the IEP of $Al_{13\text{-mer}}$ is usually found to be from 9-10, which implies the amount of base approaches B = 3, where B is the molar ratio of base to aluminum. At this point all cationic sites including ones have been neutralized, and until then, positive charge should still be exhibited. It is possible that a sample could have formed $Al(OH)_3$ from $Al_{13\text{-mer}}$ in a basic environment and yet still exhibit a positive surface charge.[3]

2.2 Background on Size Exclusion Chromatography (SEC)

Though in our work we refer to the aluminum peaks through typical size-exclusion chromatography methods as peaks L, A, K, and S, a common designation for the Al peaks in SEC is as Peaks 1-5, or 'P#', which have been characterized in recent literature,[1,2,4–8] mainly through coupled HPLC with elemental analysis and purification techniques. For example, in previous work, SEC was a preliminary screening tool in our work to crystallize the $\gamma-Al_{13\text{-mer}}$ molecule.[9] Peak 5 (S) contains small moieties that are smaller than Keggin structures, including $AlCl_3$ momoners, dimers, and the Al_{8-mer}. Peak 4 (K) species are primarily Keggin clusters. Metathesized ε-$Al_{13\text{-mer}}$ SO_4 crystals, as well as ε-$Al_{13\text{-mer}}$,δ-$Al_{30\text{-mer}}$,γ-$Al_{13\text{-mer}}$ species all fall under this peak as well. Furthermore, work[5]

with solid state ^{27}Al MAS-NMR showed that Peak 3 (A) contains species that are 'loosely' bound together, through strong external interactions, while Peak 2 (L) contains species that are more covalently agglomerated and likely non-separable. No crystal structure has ever been found for species larger than Peak 4.

Note that peak area obtained by SEC is not directly equivalent to concentration, but requires the refractive index increment (dn/dc) value of a pure species or the change in refractive index increment, which can be hard to deduce due to unresolved polydispersity of species. Different solutions under a particular peak can yield different dn/dc values, for instance.

2.3 Nuclear Magnetic Resonance Spectroscopy

A diffusion ordered nuclear magnetic resonance (NMR) spectroscopy (DOSY) experiment was carried out to see if information regarding the relative size of arginine-Al complexes could be elucidated, as in earlier work.[10] The results are seen in Supplemental Figure 4. The samples were prepared as the NMR sample in the main text, where a 1:1 [Ca]:[Arg] and 1.2:1 [Ca]:[Al] molar ratio was used, and the sample was run shortly after preparation. DOSY data was collected with a 600 MHz Varian 5mm probe. Samples were collected at 295 $^{\circ}$K. The experiments were performed by using the Gradient Stimulated Echo with Spin-Lock and Convection Compensation (DgsteSL_cc) pulse sequence. All Varian Software default settings were employed in the DOSY experiments with these exceptions: the diffusion delay was increased to 100 ms, the number of increments was increased to 25, the lowest gradient value was set to 1000, and the highest gradient value was set to 30000 (gradient values are unitless in the Varian Software on an arbitrary scale provided by a digital-to-analogue converter). These gradient values correspond to 2.1 and 62.1 G cm^{-1}, respectively. DOSY NMR data was processed

by using VNMRJ software.

The DOSY results were not able to distinguish complexed or uncomplexed forms of arginine within the solution. The size ratio between arginine and water molecules (r_{Arg}/r_{H_2O}, independent of viscosity) is much less than what was seen in previous work, and different arginine molecules have essentially the same diffusion coefficient. It is possible that more detailed information regarding the different ligand interactions could be extracted from this system (i.e. at variable temperatures or concentrations), but this is beyond the scope of this work. It is also possible that after prolonged heating, more distinct arginine-Al complexation could be seen. However, this does not appear to be vital to the initial stabilization of the system, possibly indicating that this is not a factor in the short term stability of the system. In addition to the spectra of the initial sample,

Supplemental Fig. 4 DOSY results for a NAS_{13} sample. The molar ratio of [Ca]:[Arg]:[Al] for the sample was 1.2:1.2:1, and the spectra was taken shortly after preparation. Some difference between the broad solvent peak and the arginine peaks was able to be seen, but not at the magnitude seen in other work, and with no strong difference between arginine peaks.

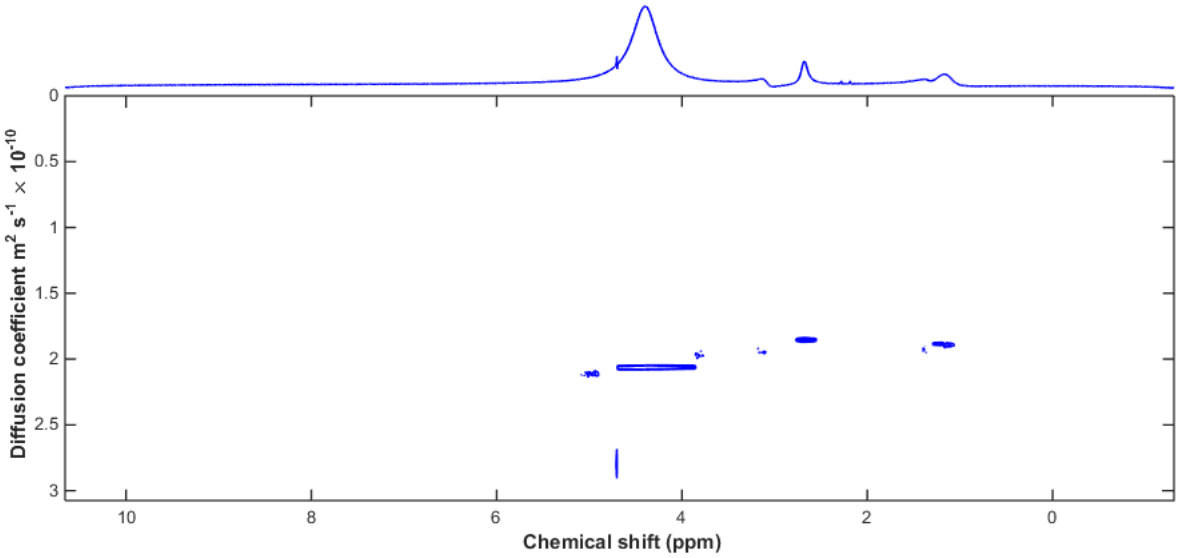

we looked at some aged/thermal treated samples with ^{27}Al NMR. In particular, samples

that had molar [Arg]:[Ca] ratios of 0.57 (gel-like), 1.07, and 1.73, and were heated for 3 days at 50 °C were analyzed. The T_d regions of these are seen in Supplemental Figure 5. Despite different ratios of [Arg]:[Ca], the species all exhibit similar peaks to the fresh sample, with a lack of the resonance at 72 ppm. Methodology for obtaining the NMR spectra is given in the main text.

Supplemental Fig. 5 ^{27}Al NMR spectra T_d range for differing Arg:Ca ratios with $Al_{13\text{-mer}}$. Samples were heated 3 days at 50 °C. The samples were 25% w/w $Al_{13\text{-mer}}$, and $CaCl_2$ was added so that there was a 1:1.2 Al:Ca molar ratio.

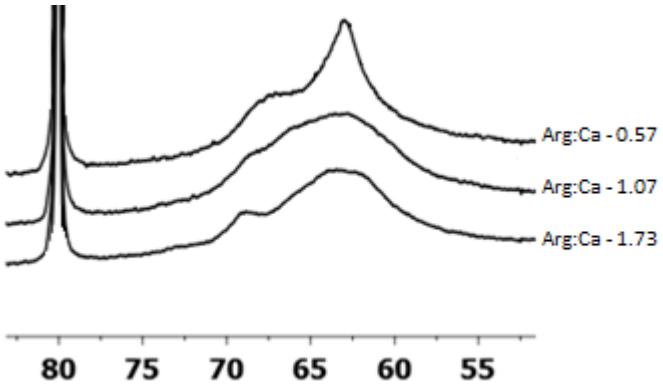

3 Details on Electronic Structure Calculations

While the fragility of this system makes it an ample candidate for applying theoretical methods, the size of the system and the complexity of the interaction is a deterrent for using more accurate techniques. In our case, we were able to perform a relatively high level *ab initio* calculation for an approximate representation of part of the system, i.e. the calcium amino-acid interaction. This interaction is interesting, and has been seen in crystal structures analogs with calcium and other amino acids, such as glycine, but has not yet been elucidated with calcium and L-arginine.

To investigate this interaction we first looked at the glycine-calcium relative ligand

binding strengths and different configurations with different conformers in the gas and solvated (implicitly) phases. We then applied the same methodology to generate different L-arginine-calcium structures. The results can be seen in Supplemental Tables 1-4 (relative enegies in 1-2, and absolute energies in 3-4). We used the wB973X functional[11,12] for geometry optimizations and the single point energy calculation, which is known to be one of the best performing hybrid functionals. To compare with this, CCSD(T), regarded as the gold standard in quantum chemistry, was used.

Qualitatively, the results for glycine and L-arginine are very similar. Gly^{-} and HArg(zw) have similar structure, and one can tell that those configurations, in particular with several calcium atoms, can be isolated as a complex. Experimentally, it is known that the glycine-Ca complexes which form are with the anionic Gly^{-} bonding with multiple calciums, which is also seen here.[13] A comparison with our results for L-arginine show similar trends, though not as strong except in structure CA10. Regardless of the exact configuration, these calculations indicate that these configurations is favorable energetically, and that complexation between calcium and L-arginine in these conditions is likely.

Supplemental Table 1 Relative energies, ΔE of the different $H_xGly_yCa_z$ complexes to standard glycine, denoted as HGly (monoprotonated). A (zw) refers to a zwitterionic configuration. A cc-pVDZ basis set was used.[14,15] Density functional theory (DFT) utilized the wB973X functional,[11,12] and CCSD(T) represents the coupled cluster singles and doubles with perturbative triples.[16,17] All calculations were done under a self-consistent reaction field, including the calcium cation. Energies in bold parenthesis are relative to deprotonated glycine. These results are more useful, as the ligand binding energy of H^+ can vary significantly in the solvent field. O_1 refers to the carboxylate oxygen closest to the amine group, whereas O_2 refers to the further carboxylate oxygen (not the diatomic). Results with a $*$ did not converge with standard CCSD(T) active space, and so a larger space was used, leading to an energy which is not quite comparable.

n	Configuration	Ligand Bonding	ΔE(DFT) kcal mol^{-1}	ΔE(CCSD(T)) kcal mol^{-1}
CG1	HGly	-	0.0	0.0
CG2	HGly(zw)	-	6.0	7.9
CG3	HGly	N-Ca-O_1	-11.5	-7.5
CG4	HGly	O_1-Ca-O_2	-19.7	-5.3
CG5	HGly	O_2	-14.0	-8.7
CG6	HGly	N-Ca-O_1,O_2-Ca	-16.0	-9.8
CG7	HGly(zw)	O_1-Ca, O_2-Ca	-27.2	-7.8
CG8	HGly	N-Ca-O_1-Ca-O_2-Ca	-11.5	-4.5
CG9	Gly^-	-	205.4 **(0.0)**	207.5 **(0.0)**
CG10	Gly^-	N-Ca-O_1	163.4 **(-42.0)**	106.6 **(-100.9)***
CG11	Gly^-	N-Ca-O_1-Ca-O_2	142.3 **(-63.2)**	165.4 **(-42.1)**
CG12	Gly^-	N-Ca-O_1-Ca-O_2-Ca	137.8 **(-67.6)**	162.5 **(-45.0)**

Supplemental Table 2 Relative energies, ΔE of the different $H_xArg_yCa_z$ complexes to standard L-arginine, denoted as HArg (monoprotonated). A (zw) refers to a zwitterionic configuration between the carboxylate and guanidine groups, whereas $(zw)_2$ is between the carboxylate and amine groups. A cc-pVDZ basis set was used.[14,15] Density functional theory (DFT) utilized the wB973X functional,[11,12] and CCSD(T) represents the coupled cluster singles and doubles with perturbative triples.[16,17] All calculations were done under a self-consistent reaction field, including the calcium cation. Energies in bold parenthesis are relative to protonated glycine. O_1 refers to the carboxylate oxygen closest to the amine group, whereas O_2 refers to the further carboxylate oxygen. $Ca_\perp$ indicates that the calcium is bound perpendicular to the plane of the carboxylate. Results with a $*$ did not converge with standard CCSD(T) active space, and so a larger space was used, leading to an energy which is not quite comparable.

n	Configuration	Ligand Bonding	E(DFT) kcal mol^{-1}	ΔE(CCSD(T)) kcal mol^{-1}
CA1	HArg	-	0.0	0.0
CA2	HArg(zw)	-	1.9	7.4
CA3	HArg(zw_2)	-	-4.6	-2.9
CA4	HArg	N-Ca-O_1	-16.2	-9.6
CA5	HArg(zw)	N-Ca-O_1	-38.4	-84.14*
CA6	HArg	O_1-Ca-O_2	-24.1	-7.5
CA7	HArg(zw)	O_1-Ca-O_2	-35.2	-9.1
CA8	HArg	N-Ca-O_1,O_2-$Ca_\perp$	-15.2	-7.7
CA9	HArg	N-Ca-O_1,O_2-Ca	-20.0	-11.1
CA10	HArg(zw)	N-Ca-O_1-Ca-O_2	-57.2	-31.0
CA11	H_2Arg^+	-	-202.3 **(0.0)**	-199.2 **(0.0)**
CA12	H_2Arg^+	N-Ca-O_1	-212.1 **(-9.8)**	-204.5 **(-5.7)**
CA13	H_2Arg^+	O_2-Ca	-214.6**(-12.3)**	-206.2 **(-7.1)**

Supplemental Table 3 Absolute energies, in Hartrees, of the different $H_xGly_yCa_z$ complexes. Conventions are similar to Supplemental Table 1. A cc-pVDZ basis set was used.[14,15] Density functional theory (DFT) utilized the wB973X functional,[11,12] and CCSD(T) represents the coupled cluster singles and doubles with perturbative triples.[16,17] All calculations were done under a self-consistent reaction field, including the calcium cation. Energies in bold parenthesis are relative to deprotonated glycine. These results are more useful, as the ligand binding energy of H^+ can vary significantly in the solvent field. O_1 refers to the carboxylate oxygen closest to the amine group, whereas O_2 refers to the further carboxylate oxygen. Results with a $*$ did not converge with standard CCSD(T) active space, and so a larger space was used, leading to an energy which is not quite comparable. Ligand energies under a solvent field for Ca^{2+} and H^+ are included as well. The ligand energy of H was derived from the average dissociation of hydronium and water under a solvent field, forming water and hydroxide, respectively.

n	Configuration	Ligand Bonding	E(DFT), H	E(CCSD(T)), H
CG1	HGly	-	-284.377013434	-283.70911057
CG2	HGly(zw)	-	-284.367510863	-283.6965279
CG3	HGly	N-Ca-O_1	-961.866961486	-960.42607697
CG4	HGly	O_1-Ca-O_2	-961.88002392	-960.42241692
CG5	HGly	O_2	-961.870960695	-960.42795318
CG6	HGly	N-Ca-O_1,O_2-Ca	-1639.34556642	-1637.1346317
CG7	HGly(zw)	O_1-Ca, O_2-Ca	-1639.36345844	-1637.1314255
CG8	HGly	N-Ca-O_1-Ca-O_2-Ca	-2316.81001767	-2313.8310939
CG9	Gly^-	-	-283.884699617	-283.21350561
CG10	Gly^-	N-Ca-O_1	-961.42316955	-960.07926647*
CG11	Gly^-	N-Ca-O_1-Ca-O_2	-1638.92849765	-1636.6904626
CG12	Gly^-	N-Ca-O_1-Ca-O_2-Ca	-2316.40714009	-2313.3999798
Ca	2+	-	-606.416207617	-604.91753187
H	1+	-	-0.16496738890	-0.1649744800

Supplemental Table 4 Absolute energies, in Hartrees, of the different $H_xArg_yCa_z$ complexes. Conventions are similar to Supplemental Table 2. A cc-pVDZ basis set was used.[14,15] Density functional theory (DFT) utilized the wB973X functional,[11,12] and CCSD(T) represents the coupled cluster singles and doubles with perturbative triples.[16,17] All calculations were done under a self-consistent reaction field, including the calcium cation. Energies in bold parenthesis are relative to protonated glycine. O_1 refers to the carboxylate oxygen closest to the amine group, whereas O_2 refers to the further carboxylate oxygen. $Ca_\perp$ indicates that the calcium is bound perpendicular to the plane of the carboxylate. Results with a $*$ did not converge with standard CCSD(T) active space, and so a larger space was used, leading to an energy which is not quite comparable. Ligand energies under a solvent field for Ca^{2+} and H^+ are included as well. The ligand energy of H was derived from the average dissociation of hydronium and water under a solvent field, forming water and hydroxide, respectively.

n	Configuration	Ligand Bonding	E(DFT), H	E(CCSD(T)), H
CA1	HArg	-	-606.416207617	-604.91753187
CA2	HArg(zw)	-	-606.413157551	-604.90576375
CA3	HArg(zw_2)	-	-606.423579118	-604.92213305
CA4	HArg	N-Ca-O_1	-1283.91352	-1281.6377706
CA5	HArg(zw)	N-Ca-O_1	-1283.94904471	-1281.7565598 *
CA6	HArg	O_1-Ca-O_2	-1283.92615684	-1281.6344042
CA7	HArg(zw)	O_1-Ca-O_2	-1283.94383678	-1281.6370165
CA8	HArg	N-Ca-O_1,O_2-$Ca_\perp$	-1961.38363151	-1958.3397206
CA9	HArg	N-Ca-O_1,O_2-Ca	-1961.39125233	-1958.3450423
CA10	HArg(zw)	N-Ca-O_1-Ca-O_2	-1961.4505086	-1958.3768109
CA11	H_2Arg^+	-	-606.903612233	-605.39946597
CA12	H_2Arg^+	N-Ca-O_1	-1284.39080971	-1282.1135004
CA13	H_2Arg^+	O_2-Ca	-1284.39474552	-1282.1157252
Ca	2+	-	-606.416207617	-604.91753187
H	1+	-	-0.16496738890	-0.1649744800

Notes and references

[1] I. Pappas, J. Vaughn and L. Pan, *Aluminum salt containing high percentage of Al_{30}*, 2012.

[2] V. Dubovoy, M. Stranick, L. Du-Thumm and L. Pan, *Cryst. Growth Des.*, 2016, **16**, 1717–1724.

[3] Z. Chen, Z. Luan, Z. Jia and X. Li, *J. Mat. Sci.*, 2009, **44**, 3098–3111.

[4] Z. Li and M. Rerek, *Stable buffered aluminum compositions having high hplc bands iii and iv containing calcium/strontium*, 2007.

[5] B. L. Phillips, J. S. Vaughn, S. Smart and L. Pan, *J. Colloid. Interf. Sci.*, 2016, **476**, 230–239.

[6] I. Pappas and L. Pan, *Antiperspirant active compositions containing aluminum salts*, 2012.

[7] L. Pan, *Antiperspirant active compositions having sec chromatogram exhibiting high sec peak 4 intensity*, 2009.

[8] J. Fitzgerald and A. Rosenberg, *Antiperspirants and Deodorants*, Markel Dekker, New York, 2nd edn, 1999, ch. 3, pp. 83–134.

[9] S. E. Smart, J. Vaughn, I. Pappas and L. Pan, *Chem. Commun.*, 2013, **49**, 11352–11354.

[10] A. F. Oliveri, C. A. Colla, C. K. , Perkins, N. Akhavantabib, J. R. Callahan, C. D. Pilgrim, S. E. Smart, P. H.-Y. Cheong, L. Pan and W. H. Casey, *Chem.-Eur. J.*, 2016, **22**, 18637–18637.

[11] J. D. Chai and M. Head-Gordon, *J. Chem. Phys.*, 2008, **128**, 084106.

[12] S. Grimme, *J. Comput. Chem.*, 2006, **27**, 1787–1799.

[13] S. Fox, I. Büsching, W. Barklage and H. Strasdeit, *Inorg. Chem.*, 2007, **46**, 818–824.

[14] D. E. Woon and T. H. Dunning, *The J. Chem. Phys.*, 1993, **98**, 1358–1371.

[15] T. H. Dunning and T. H. Dunning, *J. Chem. Phys.*, 1989, **90**, 1007–1023.

[16] G. D. Purvis and R. J. Bartlett, *J. Chem. Phys.*, 1982, **76**, 1910–1918.

[17] J. A. Pople, M. Head-Gordon and K. Raghavachari, *J. Chem. Phys.*, 1987, **87**, 5968–5975.